Send Orders for Reprints to reprints@benthamscience.net

Current Genomics, 2020, *21*, 295-310

RESEARCH ARTICLE

Functional Characterization of Alr0765, A Hypothetical Protein from *Anabaena* PCC 7120 Involved in Cellular Energy Status Sensing, Iron Acquisition and Abiotic Stress Management in *E. coli* Using Molecular, Biochemical and Computational Approaches

Antra Chatterjee[1], Shilpi Singh[1], Ruchi Rai[1], Shweta Rai[1] and L.C. Rai[1,*]

[1]*Molecular Biology Section, Centre of Advanced Study in Botany, Institute of Science, Banaras Hindu University, Varanasi-221005, India*

Abstract: ***Background*:** Cyanobacteria are excellent model to understand the basic metabolic processes taking place in response to abiotic stress. The present study involves the characterization of a hypothetical protein Alr0765 of *Anabaena* PCC7120 comprising the CBS-CP12 domain and deciphering its role in abiotic stress tolerance.

***Methods*:** Molecular cloning, heterologous expression and protein purification using affinity chromatography were performed to obtain native purified protein Alr0765. The energy sensing property of Alr0765 was inferred from its binding affinity with different ligand molecules as analyzed by FTIR and TNP-ATP binding assay. AAS and real time-PCR were applied to evaluate the iron acquisition property and cyclic voltammetry was employed to check the redox sensitivity of the target protein. Transcript levels under different abiotic stresses, as well as spot assay, CFU count, ROS level and cellular H2O2 level, were used to show the potential role of Alr0765 in abiotic stress tolerance. *In-silico* analysis of Alr0765 included molecular function probability analysis, multiple sequence analysis, protein domain and motif finding, secondary structure analysis, protein-ligand interaction, homologous modeling, model refinement and verification and molecular docking was performed with COFACTOR, PROMALS-3D, InterProScan, MEME, TheaDomEx, COACH, Swiss modeller, Modrefiner, PROCHECK, ERRAT, MolProbity, ProSA, TM-align, and Discovery studio, respectively.

***Results*:** Transcript levels of *alr0765* significantly increased by 20, 13, 15, 14.8, 12, 7, 6 and 2.5 fold when *Anabaena* PCC7120 treated with LC_{50} dose of heat, arsenic, cadmium, butachlor, salt, mannitol (drought), UV-B, and methyl viologen respectively, with respect to control (untreated). Heterologous expression resulted in 23KDa protein observed on the SDS-PAGE. Immunoblotting and MALDI-TOF-MS/MS, followed by MASCOT search analysis, confirmed the identity of the protein and ESI/MS revealed that the purified protein was a dimer. Binding possibility of Alr0765 with ATP was observed with an almost 6-fold increment in relative fluorescence during TNP-ATP binding assay with a λ max of 538 nm. FTIR spectra revealed modification in protein confirmation upon binding of Alr0765 with ATP, ADP, AMP and NADH. A 10-fold higher accumulation of iron was observed in digests of *E. coli* with recombinant vector after induction as compared to control, which affirms the iron acquisition property of the protein. Moreover, the generation of the redox potential of 146 mV by Alr0765 suggested its probable role in maintaining the redox status of the cell under environmental constraints. As per CFU count recombinant, *E. coli* BL21 cells showed about 14.7, 7.3, 6.9, 1.9, 3 and 4.9 fold higher number of colonies under heat, cadmium ($CdCl_2$), arsenic (Na_3AsO_4), salt (NaCl), UV-B and drought (mannitol) respectively compared to pET21a harboring *E. coli* BL21 cells. Deterioration in the cellular ROS level and total cellular H_2O_2 concentration validated the stress tolerance ability of Alr0765. *In-silico* analysis unraveled novel findings and attested experimental findings in determining the role of Alr0765.

***Conclusion*:** Alr0765 is a novel CBS-CP12 domain protein that maintains cellular energy level and iron homeostasis which provides tolerance against multiple abiotic stresses.

ARTICLE HISTORY

Received: January 28, 2020
Revised: March 27, 2020
Accepted: March 30, 2020

DOI:
10.2174/1389202921999200424181239

Keywords: *Anabaena* PCC7120, hypothetical proteins, adenosyl ligand binding, redox-active protein, iron homeostasis, abiotic stress management.

1. INTRODUCTION

Acclimatization to abiotic stresses enables cyanobacteria, an oxygenic photoautotroph and major contributor of global net primary production, to survive under fluctuating environmental conditions. Proteome profiling of cyanobacteria subjected to different abiotic stresses revealed the up-regulation of several hypothetical proteins with conserved domains that registered their putative role in abiotic stress tolerance [1]. Understanding of protein dynamics in metabolic rearrangements during abiotic stress mitigation requires integrative computational and wet-lab approaches. CBS-

*Address correspondence to this author at the Molecular Biology Section, Centre of Advanced Study in Botany, Institute of Science, Banaras Hindu University, Varanasi-221005, India; Tel/Fax: +91- 542-2368174;
E-mails: lcrbhu15@gmail.com; lcrai@bhu.ac.in

1389-2029/20 $65.00+.00

CP12 fusion proteins exclusively found in cyanobacteria to date hold evolutionary significance and their up-accumulation during stress provides wide scope to understand the abiotic stress tolerance mechanism. Bioinformatics analysis revealed the presence of proteins with CBS domain C-terminally fused to the CP12 domain in 126 cyanobacterial genomes [2].

Cystathionine beta synthase (CBS) domain is found to be associated with varied functions including binding with adenosyl ligands [3], gating of the osmoregulatory proteins [4], transport and binding of Mg [5], modulation of intracellular trafficking of chloride channels [6], nitrate transport [7], and 'internal inhibitors' of the pyrophosphatase activity [8] together with a noticeable presence in all forms of life suggests their evolutionary significance [9]. Several CBS domain proteins are known to participate in abiotic stress tolerance and help in the stress regulation in *Oryza sativa* and *Arabidopsis*. Microarray expression data analysis suggested the role of CBS domain-containing proteins (CDCPs) in stress response/tolerance in *Arabidopsis* [10]. Two *Arabidopsis thaliana* proteins, CBSX1 and CBSX2, are known to activate thioredoxin and, in turn, help to regulate H_2O_2 levels in the cell and hence modulate plant development and growth [11]. Singh [12] found that OsCBSX4 was regulated by stress, and its overexpression in model tobacco (*Nicotiana tabacum*) plants resulted in enhanced tolerance against various abiotic stresses such as salinity, heavy metals, and oxidative stress. OsBi1 is a CBS-containing gene that is implicated in the resistance of rice plants to brown planthoppers and responds to biotic and abiotic stress [13].

CP12 (~80 amino acid) domain-containing proteins are mostly found in cyanobacteria, algae, and higher plants [14-16]. Gene encoding CP12 or CP12-like proteins are found in all cyanobacterial genomes sequenced so far except *Cyanobacterium* sp. UCYN-A and *Moorea producta* 3L [17]. CP12 basically comprises AWD_VEEL core and two N-terminal and C-terminal redox-sensitive cysteine pairs involved in building disulfide bridges under oxidizing conditions required for the inactivation of Calvin cycle enzymes which are otherwise activated *via* thioredoxin mediated reduction that leads to CO_2 fixation [18]. Thioredoxin based regulatory system assures active carbon fixation during the day and nil during the night in oxygen phototrophs [19]. Marri [20] suggested the involvement of CP12 domain in the protection of enzymes involved in the Calvin cycle under oxidative stress in *Arabidopsis thaliana* and *Chlamydomonas reinhardtii*. The involvement of both the CBS and CP12 domains individually in abiotic stress tolerance in other organisms further gives an insight into the critical role played by such protein in the survival of cyanobacteria under extreme conditions. The energy sensing efficiency of CBS, together with the redox-sensitive cysteine residues of CP12 in a single protein, probably helped cyanobacteria in converting the earth's atmosphere from reductive to oxidative.

The present report comprises functional characterization of a hypothetical protein from *Anabaena* PCC7120 with CBS fused CP12 domain and its involvement in abiotic stress tolerance as well as in iron acquisition.

2. MATERIALS AND METHODS

2.1. Growth Conditions

Growth conditions and bacterial strains used in the experiments are similar to Rai [21]. For iron acquisition studies, *Anabaena* PCC7120 was transferred from a BG-11 medium into 50 ml YBG11 [22] containing 10 μM FeEDTA and grown at 30°C with constant shaking. After 24 h of growth, the culture was collected, washed three times with YBG11 iron-depleted media and transferred to YBG11 iron-depleted media. To minimize iron contamination, glass Erlenmeyer flasks were washed with hydrochloric acid (10%) prior to use. Before every uptake experiment, the culture was collected and washed three times with YBG11 iron-depleted media with the addition of 16 μM EDTA. In the case of *E. coli*, iron-depleted M9 minimal medium was prepared by treating M9 minimal medium with Chelex 100 resin for 1 h at room temperature (Bio-Rad) followed by supplementation with D-glucose, $MgSO_4$, and $CaCl_2$ as per [23].

2.2. Transcript Analysis of *alr0765*

To analyze the transcript level of *alr0765,* total RNA was extracted using RNASure mini kit (Nucleo-pore) from 100 mL culture (OD_{750} nm 0.6) of *Anabaena* PCC7120 treated with LC_{50} dose of arsenic (40 mM for 24 h) [24], salt (100 mM for 24 h) [25], heat (42°C for 1 h) [26], UV-B (12.9 $mWcm^{-2}$ for 30 min) [27], drought (30°C for 24 h) [28], butachlor (32μM for 24 h) [29], cadmium (10 μM for 24 h) [30] and methyl viologen (2 μM for 6 h) [31] and without treatment (control). cDNA from RNA was prepared using the iScript cDNA synthesis kit (BioRad). Primer3 software was used to design gene-specific primer sets: 5' CTGGAACAGCCCTACACCAT 3' and 5' TGCTAACTTTTTC GGCTCGT 3' for *alr0765* and for reference *16S rRNA* gene: 5' CACACTGGGACTGAGACAC 3' and 5' CTGCTGGCACGGAGTTAG 3' and *rnpB* gene: 5'TAGGGAGAGA GTAGGCGTTG 3' and 5'TTCTGTGGCACTATCCTCA C3'. 25 ng of cDNA extracted from each sample was used for quantitative real-time PCR (qRT-PCR). Reactions were performed in 96-well plate in triplicate using a total volume of 20 μl, including 10 pmol of forward and reverse primers and 1x SsoFast EvaGreen qPCR supermix (BioRad). Transcript levels were normalized to 16S transcript and rnpB transcript and the relative expression ratio of *alr0765* gene was calculated using the comparative Cq value method according to the BioRad manual [29]. Melting curve analysis of the amplified products was employed for the specificity of the real-time PCR. $FeCl_3$ stock solution (5 mM in 10 mM citric acid, 10 mL) was prepared and applied to *Anabaena* PCC7120 as 0.1 μM, 0.5 μM, 1 μM, 3 μM and 5 μM while cDNA was isolated using the same protocol as mentioned above. In the case of *E. coli,* 3.5 μM was added after induction in *E. coli* and the cDNA was isolated as per the above protocol.

2.3. Cloning and Expression

Open reading frame of *alr0765* (WP_010994939.1) encoding a hypothetical protein, was amplified by polymerase chain reaction using genomic DNA as the template with a pair of primers, Pf (5'GGAATTCCATATGTTAAAAGCATCAGA CGTTATG3') and Pr (5' CCGCTCGAGATCAGTAATT-

GCATTCATT AACAC3'). The PCR was done in a reaction mixture of 25µl for 30 cycles at 94°C for 1.30 min, 55°C for 1 min, and 72°C for 2 min using standard PCR conditions. The purified *alr0765* fragment was digested with the restriction enzymes NdeI and XhoI and ligated into pET21a vector. Recombinant vector pET21a-*alr0765* was transformed into *E. coli* DH5α cells. The integrity of the recovered plasmid was confirmed by restriction digestion. For expression of the recombinant protein, the pET21a-*alr0765* plasmid was transformed into competent BL21 (DE3) cells.

2.4. Purification of Recombinant Protein Alr0765

20 mL overnight grown culture of BL21 (DE3) *E. coli* containing the recombinant plasmid pET-21a-*alr0765* was inoculated in fresh 1000 ml LB broth containing 100 µg ml^{-1} ampicillin and incubated at 37°C for 4 h (or till OD_{600} reached ~ 0.6). The cultures were induced with a final concentration of 0.5 mM IPTG by incubating at 37°C for 4 h and shaking at 180 rpm. Following induction, overexpressed cells were harvested and washed with milli-Q water. The cell pellets were suspended in lysis buffer comprising 10 mM Na_2HPO_4, 2.7 mM KCl, 140 mM NaCl, 1.8 mM KH_2PO_4, pH 7.5 and disrupted by crushing in the presence of 10 µM PMSF (Sigma) with liquid nitrogen. The soluble fraction was obtained after centrifugation at 4°C and 15000 rpm for 45 minutes. Supernatant having recombinant His tagged fusion protein was loaded at 1 ml/min flow rate onto a 5-ml Ni-NTA column (GE Healthcare) pre-equilibrated with the binding buffer (20 mM sodium phosphate, 0.5 M NaCl, 5 mM imidazole, pH 7.5). The column was then washed with a 25-ml binding buffer followed by elution with 5-ml elution buffer (20 mM sodium phosphate, 0.5 M NaCl, 0.5 M imidazole, pH 7.5). Protein purity was determined by using 12% sodium dodecyl sulfate polyacrylamide gel electrophoresis (SDS-PAGE) followed by western blotting. The purified protein was subjected to MALDI-TOF MS/MS analysis for confirmation of its identity [32]. Electrospray mass spectrometry (ESI-MS) analysis was performed (2.5 mg/ml protein) to analyze the dimerization of protein as per Banerjee [33].

2.5. Fourier Transform Infrared Spectroscopy (FTIR) for Ligand Binding Analysis

Fourier transform infrared spectroscopy was used to record infrared spectra (600 spectral scans) in an FTIR spectrum recorded on ALPHA BRUKER Eco-ATR. Samples were placed in a cell with CaF_2 windows and 100-µm Teflon spacer. For infrared amide I band recordings, 400 mg of protein in Tris buffer, pH 8.0 or in ligand buffer containing 10 mM HEPES, 10 mM MOPS, 10 mM CAPS, 10 mM potassium acetate, 100 mM KCl and adenosyl-ligands, *viz*., ATP or ADP or AMP or NADH at pH 8.0 was taken as per Martinez-Cruz [34]. Sample volumes were reduced to about 20 ml by filtration on Vivaspin concentrator. The concentrated samples were dehydrated and vacuum evaporated in a speedvac and resuspended in 20 µl of D_2O. For the samples (1.3 mM protein) in the presence of adenosyl-derivatives, the final concentrations of the ligands (ATP, ADP, AMP, NADH, GAPDH, PRK) were 3 mM. Fourier self deconvolution and derivation analysis were performed with Origin Pro8 SR0.

2.6. Atomic Absorption Spectroscopy (AAS) and Energy Dispersive X-ray Spectroscopy (EDS) for Metal Analysis

For quantitative measurement of iron, the purified protein was concentrated in speedvac and denatured at 70°C for 1 hour and allowed for metal content analysis with atomic absorption spectrometry (Perkin-Elmer; A Analyst 600) fitted with graphite furnace, and the amount was calculated using a reference standard provided by Accustandard, USA [35]. For EDS analysis of purified protein, a film of the concentrated sample was prepared on the copper strip and analyzed by scanning electron microscopy (Zeiss EVO18 SEM), and spectra of metal were obtained by energy-dispersive X-ray spectroscopy (INCA-EDS SOFTWARE) instrument.

2.7. Cyclic Voltammetry to Check Redox Activity of Protein

Cyclic voltammetry of the native protein (50 mM) at pH 7.5 was measured as per Nishio *et al.*, [36] using the electrochemical cell with the ITO ($3cm^3$) glass as the working electrode, the platinum wire as the counter electrode, and the Ag/AgCl electrode (saturated KCl) as the reference electrode at temperature 16°C. The measurements were carried out in a potential range of −0.4 V to +0.8 V (*vs* Ag/AgCl) using CHI 630C Series (USA) Electrochemical system.

2.8. Reactive Oxygen Species (ROS) Generation Analysis

Intracellular oxidation in terms of ROS generation was measured under different stresses [37] BL21 (DE3) cells transformed with empty vector (pET-21a) or recombinant vector (pET-21a-*alr0765*) were inoculated in LB medium containing 100 µg ml^{-1} ampicillin and grown overnight. 100 µl inoculum (OD_{600} 0.6) was added into 25 ml LB medium, in the presence or absence of different stresses *viz*, Na_3AsO_4 (6 mM), $CdCl_2$ (250 µM), heat (55°C for 1 h), mannitol (desiccation) (600 mM), methyl viologen (120 µM), NaCl (800 mM) with 0.5 mM IPTG, incubated at 37°C with shaking (180 rpm) for 4 h. 5 ml of culture from each sample were centrifuged, followed by washing of the pellets and their resuspension in MOPS buffer, pH 7.5. From the stock of 10 mM H_2DCFDA (dissolved in ethanol), a final concentration of 10 µM was further added to the samples and incubated at 37°C in the dark for 30 min. ROS emission from all the cultures were measured using a Perkin-Elmer LS-5B spectrofluorimeter (excitation, 490 nm; emission, 519 nm).

2.9. Hydrogen Peroxide Concentration Measurement

Hydrogen peroxide in each sample was estimated by forming titanium-hydro peroxide complex [38]. Both empty vector (pET21a) and recombinant vector (pET21a-*alr0765*) transformed BL21 (DE3) were grown and subjected to stress, as mentioned above. 25 ml culture from each sample was centrifuged and the pellets were ground to a fine powder with the help of liquid nitrogen followed by the addition of 10 ml cold acetone. Mixtures were filtered with Whatman No. 1 filter paper followed by the addition of 4 ml titanium reagent and 5 ml ammonium solution to precipitate the titanium-hydro peroxide complex. Reaction mixtures were further centrifuged at 10,000 g for 10 min in a refrigerated centrifuge. The precipitate was dissolved in 10 ml 2 M H_2SO_4 and then re-centrifuged. Supernatant's absorption was read at

415 nm against reagent blank in a UV-visible spectrophotometer. The concentration of hydrogen peroxide was computed by referring to a standard curve made from known concentrations of hydrogen peroxide.

2.10. Measurement of Multiple Stress Tolerance by Spot Assay and CFU Method

The effect of abiotic stresses on *E. coli* BL21 (DE3) strains transformed with empty pET21a and recombinant pET21a-*alr0765* vectors were analyzed using spot assay under treatments of heat (55°C) for 1 h and 1.5 h, cadmium ($CdCl_2$) with 250 µM and 350 µM, UV-B for 10 min and 15 min, arsenic (Na_3AsO_4) with 6 mM and 8 mM, mannitol (for drought) at 0.6 M and 0.8 M and NaCl with 800 mM and 900 mM. The transformed cells were grown in LB medium supplemented with 100 µg/ml ampicillin at 37°C till the OD_{600} reached 0.6, followed by the addition of 0.5 mM IPTG and allowed to grow for 4 h at 37°C at 180 rpm. Further, the cultures were serially diluted to three levels (10^{-1}, 10^{-3}, and 10^{-5}) and 3 µl from each dilution was spotted on LB-ampicillin plates containing the above-mentioned stressors and incubated overnight at 37°C. In addition, the CFU count method was applied for quantitative analysis of the effect of abiotic stresses on transformed *E. coli* BL21 (DE3) strains using the same process for growth and IPTG induction as applied in spot assay. The bacterial count was estimated and calculated as per Agrawal [39].

2.11. Sequence Retrieval and *In-silico* Functional Prediction

To find out the homologous of Alr0765 from other species, BLAST and RCBS databases were used. Protein sequences retrieved were subjected for multiple sequence alignment using PROMALS-3D (http://www.ebi.ac.uk/). Functional annotation of target protein was done using InterProScan [40] and Motif suit MEME (http://meme-suite.org) was used for motif analysis. Molecular function prediction was performed *via* gene ontology prediction with COFACTOR from the Zhang lab using the amino acid sequence of Alr0765 [41]. COACH database was used to find out probable ligands and consensus binding residues for the protein [42].

2.12. Homology Modeling and Structure Validation

Secondary structure composition was predicted with predict protein server (www.predictprotein.org) [43]. The 3D-models of the target protein were generated using (http://swissmodel.expasy.org/) Swiss modeller [44] and refined with Modrefiner [45]. The quality of the final refined model was evaluated by Ramachandran plot analysis using PROCHECK [46] and ERRAT [47] through structure analysis and verification *via* the MolProbity server [48]. The ProSA (Protein Structure Analysis) was used to test the local and overall quality of the 3D-models developed [49]. TM-align server was used to superimpose the model structure with template and Root Mean Square Deviation (RMSD) calculations [50].

2.13. Statistical Analysis

One-way ANOVA followed by Dunnett's *post hoc* test ($p< 0.05$) was used to compare the variation between control and treatment in real-time PCR results for expression analysis as well as in case of comparison of expression between control and different concentration of iron. Student's paired *t*-test was done to analyse the notable variation in the case of iron accumulation by *E. coli* with empty vector and *E. coli* with a recombinant vector. Similarly, a student's paired *t*-test was also applied to analyze the significant difference in H_2O_2 concentration for the control and each of the stress treatments. Statistical analysis was performed using SPSS Inc. Version 16.

3. RESULTS

3.1. Transcript Analysis of *alr0765* of *Anabaena* PCC7120 Under Different Abiotic Stresses

For studying the role of *alr0765* of *Anabaena* PCC7120 under abiotic stresses, its transcript levels from unexposed (control) and those treated with LC_{50} dose of heat, arsenic (Na_3AsO_4), cadmium ($CdCl_2$), butachlor, salt (NaCl), drought (mannitol), UV-B, and methyl viologen were compared. Transcript levels of *alr0765* increased by 20, 13, 15, 14.8, 12, 7, 6 and 2.5 fold, respectively, with respect to control (Fig. **1**). One-way ANOVA revealed significant variation among control and treatments (df =8, 18; F = 10.471; $p<0.001$) for fold changes in expression of *alr0765*. Dunnett's *post hoc* test revealed significantly higher ($p<0.001$) fold change for the heat, cadmium and butachlor treatments and arsenic ($p<0.05$), thereby suggesting a crucial involvement of Alr0765 in abiotic stress management in *Anabaena* PCC7120.

3.2. Alr0765 Belongs to CBS Superfamily and Possess Adenosyl Ligand-binding Motif

Different domain search databases suggested the presence of CBS domain fused with CP12 in Alr0765 (domain architecture ID 10140279) (Fig. **S1**). It consists of 204 residues, of which about 127 N-terminal residues form a CBS pair and about 77 C-terminal residues belong to the CP12 domain (Fig. **S2**). Multiple sequence alignment of Alr0765 revealed the presence of putative adenosyl ligand binding signature sequence Ghx(T/S)x(T/S)xD [51] (Fig. **2**). The amino acids present in Alr0765 associated with a conserved signature sequence are G^{48}, S^{51}, S^{53} and D^{54}. Furthermore, target sequence analysis with MEME also revealed the signature sequence GI(I/N)S(E/L)(T/S/E)D/C as a conserved motif comprising all such conserved amino acids (Fig. **3**). Such findings indicated the functionality of the Alr0765 in adenosyl ligand binding.

3.3. Molecular Cloning of *alr0765* Gene and Heterologous Expression in *E. coli*

The 615 bp PCR amplified product was digested with NdeI and XhoI, and ligated to pET-21a vector (Fig. **S3a**) and transformed into *E. coli* BL21 (DE3) strain. Recombination of *alr0765* into pET21a was confirmed with double digestion of recombinant vector (Fig. **S3b**) and further with colony PCR. A 4 h exposure of *E. coli* BL21 (DE3) cells transformed with recombinant plasmid to 0.5 mM IPTG resulted in the induction of the heterologously expressed protein with a molecular weight of approximately 23 kDa as observed on the SDS-PAGE (Fig. **S4c**). Fig. (**S4b**) clearly demonstrated

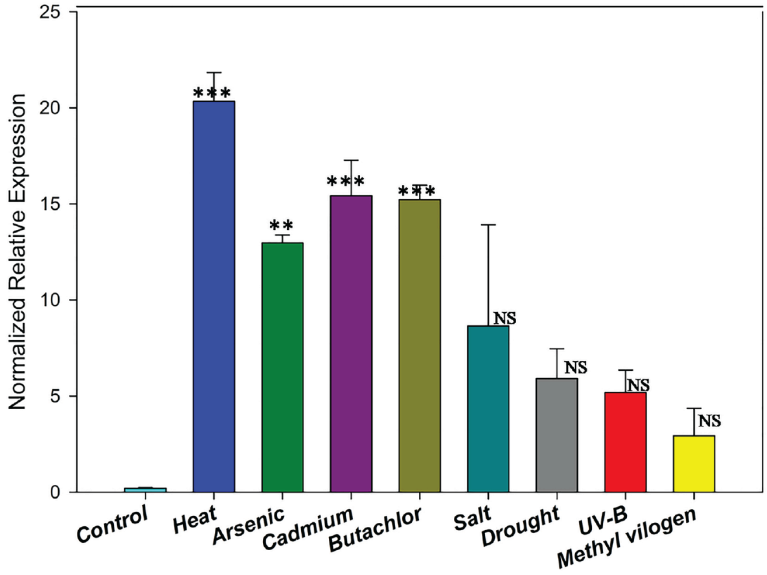

Fig. (1). qRT-PCR analysis of *alr0765* gene showing the effect of arsenic (Na_3AsO_3), cadmium ($CdCl_2$), salt (NaCl), heat (42°C), UV-B, butachlor and drought (mannitol) after 24 h on *Anabaena* PCC7120. Transcript levels were determined by qRT PCR. The 16S rRNA and rnpB genes were used as an internal control for normalizing the variations in cDNA amounts. Biological triplicates were averaged. Bars indicate SEM. One-way ANOVA followed by Dunnett's *post hoc* test. Indicators signify * P< 0.05, ** P<0.01, *** P<0.001 significant differences and NS as non-significant difference between control and treatments. (*A higher resolution / colour version of this figure is available in the electronic copy of the article*).

Fig. (2). Multiple Sequence alignment of Alr0765 with proteins containing CBS domain belong to different organisms with solved structure revealed the presence of adenosyl binding motif in a black box and the stars indicate the amino acid conserved in all the sequences. Coloured sequences represent predicted secondary structures (red: alpha-helix, blue: beta-strand). Consensus predicted secondary structure symbols: alpha-helix: h; beta-strand: e. Consensus amino acid symbols are: conserved amino acids in bold and uppercase letters; aliphatic (I, V, L): l; aromatic (Y, H, W, F): @; hydrophobic (W, F, Y, M, L, I, V, A, C, T, H): h; alcohol (S, T): o; polar residues (D, E, H, K, N, Q, R, S, T): p; tiny (A, G, C, S): t; small (A, G, C, S, V, N, D, T, P): s; bulky residues (E, F, I, K, L, M, Q, R, W, Y): b; positively charged (K, R, H): +; negatively charged (D, E): -; charged (D, E, K, R, H). (*A higher resolution / colour version of this figure is available in the electronic copy of the article*).

Fig. (3). MEME elucidated adenosyl ligand binding motif comprising signature sequence in red box. (*A higher resolution / colour version of this figure is available in the electronic copy of the article*).

a single band of about 23 kDa of purified protein from *E. coli* BL21 (DE3) on SDS-PAGE. Immunoblotting of recombinant protein with an anti-his antibody developed a single band of approximately 23 kDa, thus confirming the successful translation of the recombinant construct in the *E. coli* BL21 (DE3) (Fig. **S4 d**). MALDI-TOF-MS/MS, followed by MASCOT search analysis, confirmed the identity of the purified protein (Fig. **S5**). ESI/MS with native protein revealed dimer formation, one of the characteristics of CBS domain-containing proteins (Fig. **4**).

3.4. TNP-ATP and FTIR Assay to Analyze Protein-ligand Binding Possibilities

TNP-ATP is a fluorescent ATP analog, which has been developed as an important probe for the assessment of nucleotide-binding of various eukaryotic and bacterial proteins [52-54]. Almost 6 fold increment in relative fluorescence was observed when 200 mM TNP-ATP was incubated with an equimolar concentration of target protein with a λ max of 538 nm. After the addition of 100 mM of ATP to Alr0765: the TNP-ATP complex around the 3-fold reduction in the TNP-ATP peak at 538 nm was observed. This implies the competition expressed by unmodified ATP to the binding pockets of Alr0765 against TNP-ATP. Such findings suggested the binding possibility of ATP to Alr0765 (Fig. **5**).

Bands of the FTIR spectra obtained at pH 8.0 and temperature 25 ^{o}C were investigated for Alr0765 in the absence as well as in the presence of ATP, ADP, AMP, NADH, GAPDH and PRK. Fourier self deconvolution and derivation analysis of the amide I band revealed the maxima shown in Tables **1** and **2**. The 1633 cm^{-1} component corresponds to the intramolecular β sheet and that of 1644 cm^{-1} assigned to the random coil. 1651 cm^{-1} belongs to α helix and that of 1688 cm^{-1} attributed to turns and loops [55]. Upon ligand binding, the conformation in the secondary structure was changed as revealed from the modification of FTIR spectra in terms of alteration in different band areas correspond to different secondary structures in Table **2**. Since adenosyl moieties absorb at 1620 cm^{-1} due to in-plane vibration; therefore, changes in FTIR spectra obtained after incubating Alr0765 with different ligands may be a result of protein-ligand interaction [56]. The almost negligible difference in band areas corresponding to different secondary structures has been obtained after Alr0765 incubation with GAPDH or PRK. Therefore, the findings of TNP-ATP and FTIR assays suggested that Alr0765 binds with adenosyl ligands, which led to conformational changes, although no binding was found with GAPDH or PRK.

3.5. Computational Analysis of Alr0765 for Ligand Binding Analysis

COFACTOR revealed the probable molecular function of the target protein falls under the category of nucleotide-binding (GO:0000166) with Cscore 0.64 and ion binding (GO:0043167) with Cscore 0.61 as per gene ontology (Table **S1**). The findings of the COACH server indicated that the protein interacts with AMP, ATP, NADH, Fe as relevant ligands and their consensus binding residues are mentioned in Table **3**.

3.6. *In- silico* Secondary Structure Analysis of Alr0765

TheaDomEx server [57] using fasta sequence suggested segmentation of the amino acid sequence of Alr0765 into two parts, N terminal comprising CBS domain from residue 1-127 and C terminal comprising CP12 domain of about 77 residues long. ThreaDomEx suggested typical patterns of α-β-α-β-β-α repeated two times exhibited by N terminal part (1-127 residues long) comprising CBS domain of target protein (Fig. **S2**).

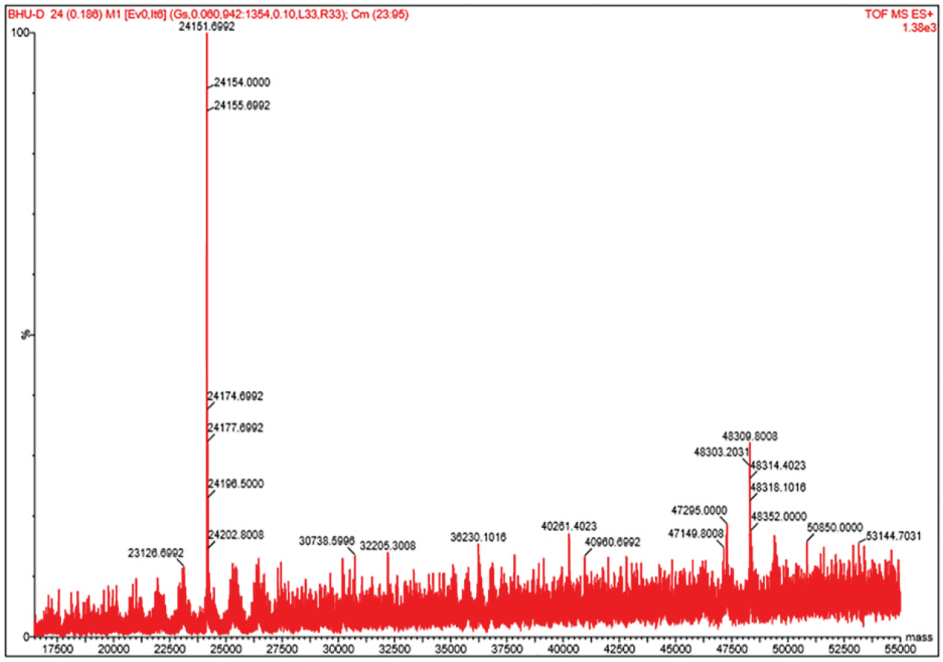

Fig. (4). ESI/MS analysis for protein dimerization. Peak at 48309.8 suggests dimer formation with monomer peak at 24151.6. (*A higher resolution / colour version of this figure is available in the electronic copy of the article*).

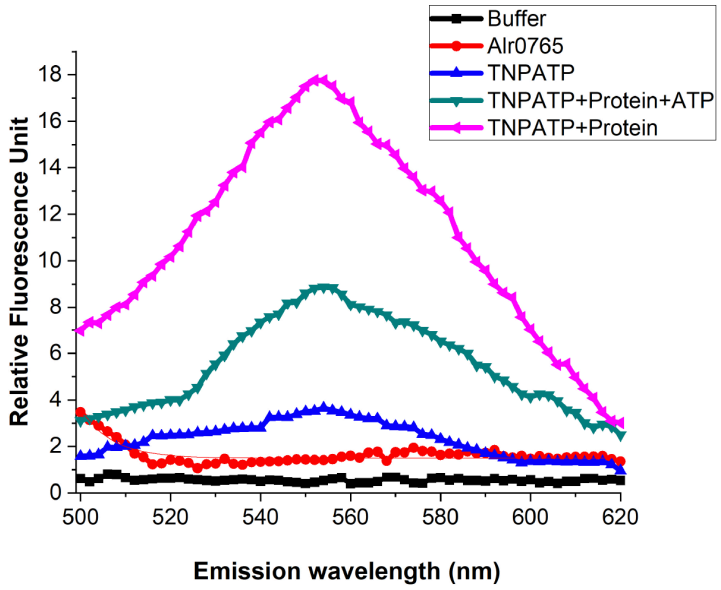

Fig. (5). Fluorescence emission spectra of TNP-ATP in the absence and presence of Alr0765 and Alr0765 incubated with ATP. Scanning emission spectra of TNP-ATP alone (blue) and in complex with Alr0765 (pink) were collected using an excitation wavelength of 403 nm, and emission wavelength from 500nm to 600 nm. (*A higher resolution / colour version of this figure is available in the electronic copy of the article*).

3.7. Homology Modeling, Model Refinement and Molecular Docking

Homology model built for Alr0765 based on the template from CBS-CP12 domain-containing protein of bloom-forming cyanobacteria with PDB ID 5NMU extracted from the RCSB database (Fig. **S5**) was further refined with modrefiner and quality was checked with Ramachandran plot analysis and Z score. Ramachandran plot displayed 97.3 % residues in favored region, 2.7 in the allowed region, and 0% in the disallowed region (Fig. **S6a**). Such values are closer to expected ratios of favored region as 98%, allowed region as 2% and disallowed as 0%. Z-score revealed -6.3 for the built model, which signifies a good quality model for its native conformation (Fig. **S6b**). Furthermore, the superimposing of the target protein model with the template model revealed the root mean square deviation of 0.24 and suggested a good model (Fig. **S6c**). Molecular docking studies of Alr0765 with AMP, ATP, ADP, and NADH indicate the involvement of residues that fall under alpha helix, beta-sheet as well as coil and turns (Fig. **6**). This suggests that the binding of adenosyl ligands with Alr0765 leads to conformational changes in Alr0765.

3.8. Iron Acquisition

In oxygenated aqueous solutions, Fe^{3+} is the most bioavailable form of iron; hence $FeCl_3$ was used to design the experiment [58]. Real-time PCR analysis revealed that in the presence of different concentrations of $FeCl_3$ *viz*., 0.1µM, 0.5µM, 1µM, 3µM, 5µM transcript levels of *alr0765* increased by 123, 87, 22.4, 21.7, and 12.7 fold respectively as compared to control (Fig. **7**). One-way ANOVA revealed significant variation among control and treatments (df =5, 12; F = 77.55; $p<0.001$) for fold changes in expression of *alr0765*. Dunnett's *post hoc* test revealed a significantly higher ($p<0.001$) fold change for the $FeCl_3$ concentrations of 0.1µl and 0.5µl (Fig. **7**). The expression of *alr0765* was doubled with IPTG induction in the presence of 3µM $FeCl_3$ in the medium containing recombinant pET-*alr0765* transformed *E. coli* as compared to IPTG induction without $FeCl_3$ (Fig. **S7**). Furthermore, AAS data results suggested that IPTG induced *E.coli* with recombinant vector accumulated 10 times higher iron as compared to uninduced *E.coli* containing recombinant vector (Fig **8A**). EDS spectrum of purified Alr0765 further supported the presence of bound iron (Fig **8B**). The above results suggested that Alr0765 involved in iron acquisition regulates cellular metabolism of *Anabaena* PCC7120.

3.9. Redox Potential Generated by Alr0765

To measure the redox potential of Alr0765, cyclic voltammetry of isolated protein was performed. CV generated potential window showed positive and negative peaks corresponding to the oxidation of Fe^{2+} to Fe^{3+} and reduction of Fe^{3+} to Fe^{2+}. The redox potential was measured from the midpoint potential between oxidation and reduction peak potentials and the potential difference generated was 146mV (Fig. **9**). This suggested that Alr0765 is a redox-active protein and might be involved in maintaining the redox status of the *Anabaena* PCC7120.

3.10. Effect of Different Abiotic Stresses on Recombinant pET-*alr0765* Transformed *E. coli* Cells Using Spot Assay and CFU Count Method

To elucidate the stress tolerance traits of *alr0765,* its heterologous expression in *E. coli* was employed. A comparative sensitivity test was performed on the agar plate using pET21a transformed *E. coli* cells as well as cells transformed with a recombinant plasmid (pET21a-*alr0765)* under different stress concentration *viz*., 6 mM and 8 mM sodium arsenate, 250 µM to 350 µM cadmium chloride, 800 mM and 900 mM sodium chloride, 0.6 M and 0.8 M mannitol, 10 and 15 min of UV-B (12.9 mW/cm^{-2}), heat ($55^{o}C$) 1 h and 1.5 h. Spots of recombinant (pET21a-*alr0765*) transformed cells were found with better growth as compared to only pET21a transformed cells (Fig. **10**). Spot assay results were

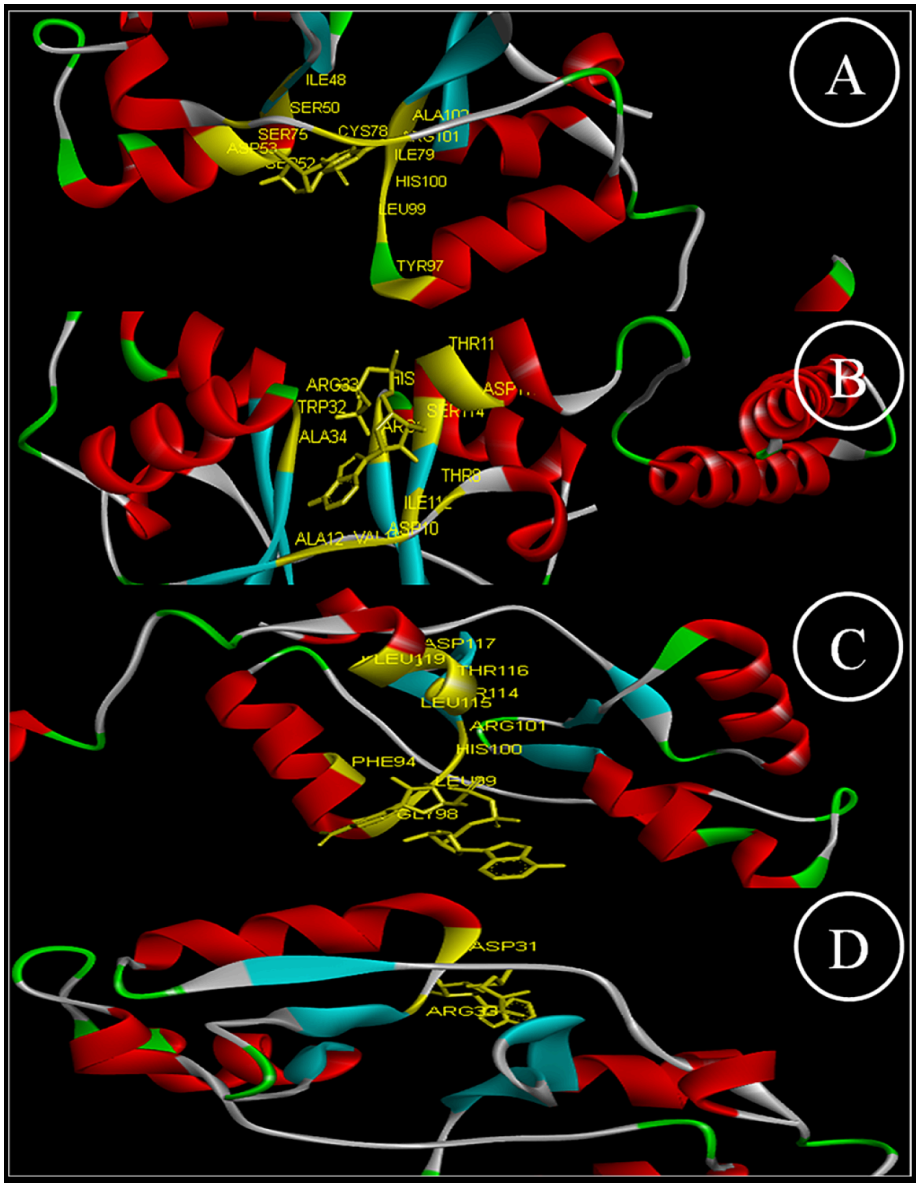

Fig. (6). Molecular docking of Alr0765 with different ligands depicting binding residues. **6a**. with AMP; **6b**. with ATP; **6c**. with ADP; **6d**. with NADH. (*A higher resolution / colour version of this figure is available in the electronic copy of the article*).

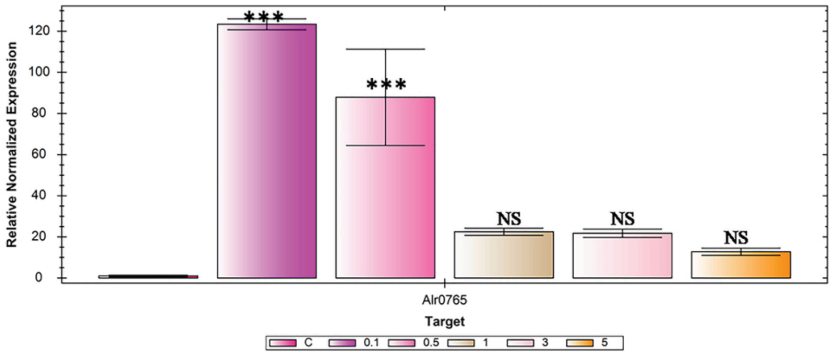

Fig. (7). Transcript level of *alr0765* in *Anabaena* PCC7120 exposed to different $FeCl_3$ concentration (0.1µM, 0.5µM, 1µM, 3µM, 5µM). The 16S rRNA and rnpB genes were used as an internal control for normalizing the variations in cDNA amounts. Biological triplicates were averaged. Bars indicate SEM. One-way ANOVA followed by Dunnett's *post hoc* test. Indicators signify * P< 0.05, ** P<0.01, *** P<0.001 significant differences and NS as non-significant difference between control and treatments. (*A higher resolution / colour version of this figure is available in the electronic copy of the article*).

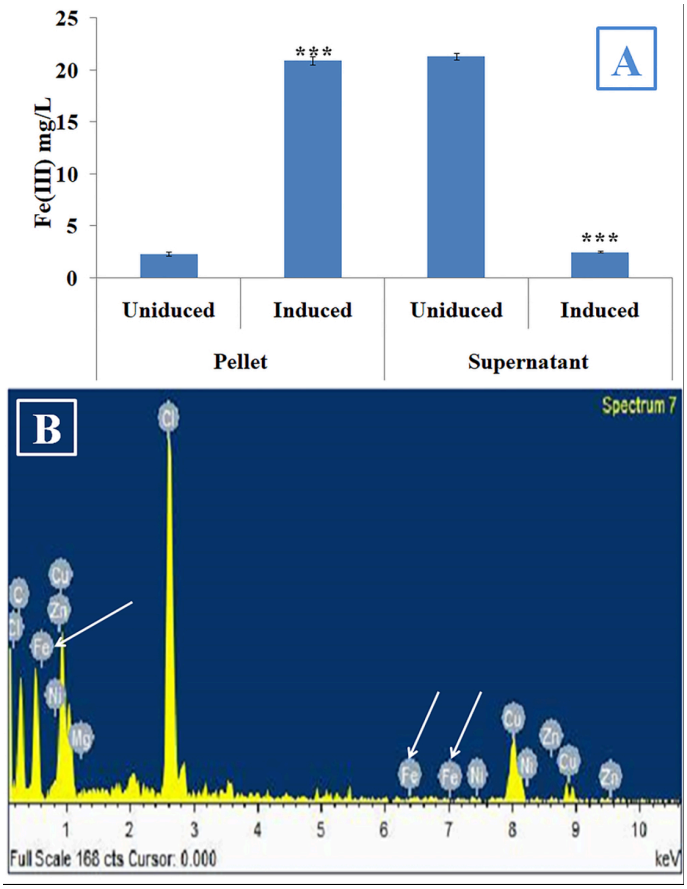

Fig. (8). Iron acquisition by Alr0765. **8A**. AAS analysis for iron accumulation revealed higher accumulation of iron in *E. coli* transformed with pET21a-*alr0765* after induction with IPTG whereas higher accumulation of iron in supernatant compared to pellet without induction. Student's paired *t*-test (***p<0.001) was used to compare Fe(III) content between uninduced and induced pellet and supernatant. **8B**. EDS spectrum of isolated Alr0765 displaying the presence of iron atom. (*A higher resolution / colour version of this figure is available in the electronic copy of the article*).

quantitatively confirmed with the CFU count method. Recombinant *E. coli* BL21 cells showed about 14.7, 7.3, 6.9, 1.9, 3, 4.9 fold higher number of colonies under heat, $CdCl_2$, Na_3AsO_4, NaCl, UV-B and mannitol respectively compared to pET21a harboring *E. coli* BL21 cells (Table **1**).

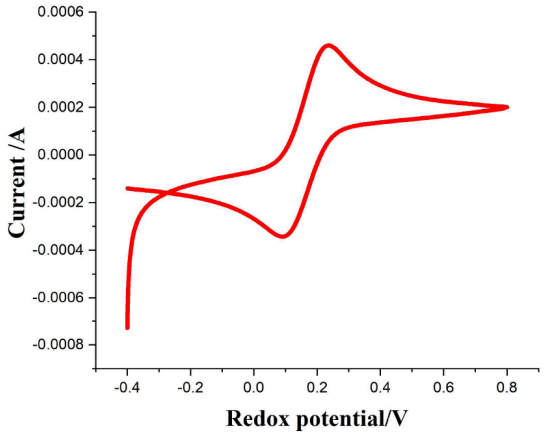

Fig. (9). Potential window generated with cyclic voltammetry for Alr0765 at a scan rate of 10mV s^{-1}. (*A higher resolution / colour version of this figure is available in the electronic copy of the article*).

3.11. Amelioration of Intracellular Oxidation in Terms of ROS Generation and H_2O_2 Concentration Measurement

To support the hypothesis that Alr0765 bears a significant role in abiotic stress tolerance, comparative ROS generation and intracellular H_2O_2 measurements were performed. In the case of ROS generation analysis, the intensity of H2DCFDA was approximately equal in both BL21 (DE3) cells transformed with a recombinant vector or empty vector in the absence of different stresses. Interestingly, the BL21/pET21a-*alr0765* cells showed a reduction in H_2DCFDA intensity by 23%, 23.4%, 54.4%, 63.9%, 47.6%, 48.3% under arsenic, cadmium, heat, mannitol, methyl viologen, and NaCl, respectively as compared to BL21/pET-21a cells under the same stresses (Fig. **11**). Assessment of intracellular H_2O_2 level also revealed marked reduction in case of recombinant vector transformed BL21 (*E. coli* 2) as compared to empty vector (*E. coli* 1) under different abiotic stresses (Fig. **12**). Almost equal basal levels of H_2O_2 concentration were observed in both types of cells grown with or without exogenous stress application (control). Statistical analysis by Student's paired sample t-test indicates that the cellular concentration of H_2O_2 (mM) was significantly greater in *E. coli* 1 than *E. coli* 2 for all the 5 treatments.

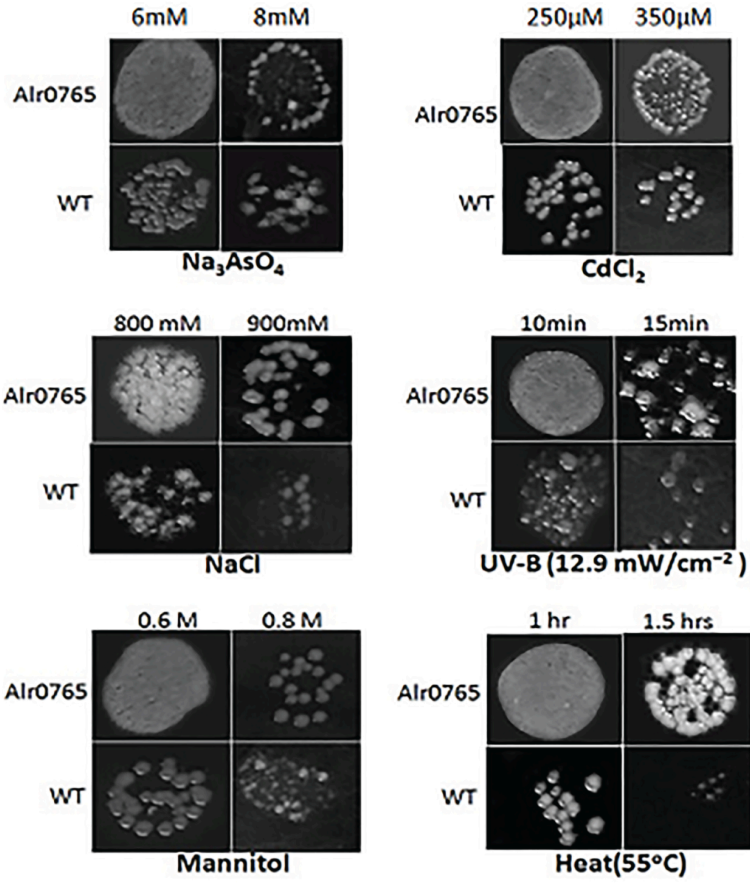

Fig. (10). Spot assay analysis to depict the stress tolerance behavior of Alr0765 when heterologous expressed in *E. coli* subjected to different abiotic stresses.

Table 1. CFU/ml of *E. coli* strain BL21 (DE3) transformed with empty vector (BL21/pET-21a) and recombinant plasmid (BL21/pET-21a- *alr0765*) under different abiotic stresses.

Stress	BL21/pET-21a-*alr0765*	BL21/pET-21a
Heat (1 h at 50°C)	50.56× 10^6	3.43× 10^6
$CdCl_2$ (250 µM)	43.25× 10^6	5.9× 10^6
Na_3AsO_4 (6 mM)	42.69× 10^6	6.11× 10^6
NaCl (800 mM)	12.56× 10^6	7.9× 10^6
UV-B (10 m) (12.9mW/cm^{-2})	25.76× 10^6	8.58× 10^6
Mannitol (600 mM)	31.24× 10^6	6.32× 10^6

4. DISCUSSION

The function of CBS proteins in cyanobacteria is still unexplored. CBS domain is known to bind with adenosyl groups of AMP, ATP [59], or s-adenosylmethionine [60], which in turn regulates the activity of associated enzymatic domains [3]. In eukaryotic cells, CBS domain-containing proteins act as a sensor of the energy status such that an increase in the cellular AMP: ATP ratio results in activation of AMPK, which then acts to inhibit energy-utilizing (anabolic) pathways and activate energy-producing (catabolic) pathways [61]. The binding of adenosyl ligands with the Alr0765 was explored with two different approaches: TNP-ATP assay and FTIR analysis (Fig. **8**, Table **2**). FTIR suggested that binding of different ligands led to an alteration in the percentage of secondary structures. Change in FTIR spectra in terms of alteration in-band areas corresponding to secondary structure taken as modification in protein confirmation has been reported in CBS domain-containing protein MJ0729 of *Methanocaldococcus jannaschii* [62]. Furthermore, multiple sequence alignment of Alr0765 with proteins from different organisms having adenosyl binding signature sequence (Fig. **2**) as well as motif elucidation of Alr0765 (Fig. **3**) also supported its probable role in adenosyl ligand binding. The docking study further attested the binding of Alr0765 with different adenosyl ligands (Fig. **9**) and the binding residues

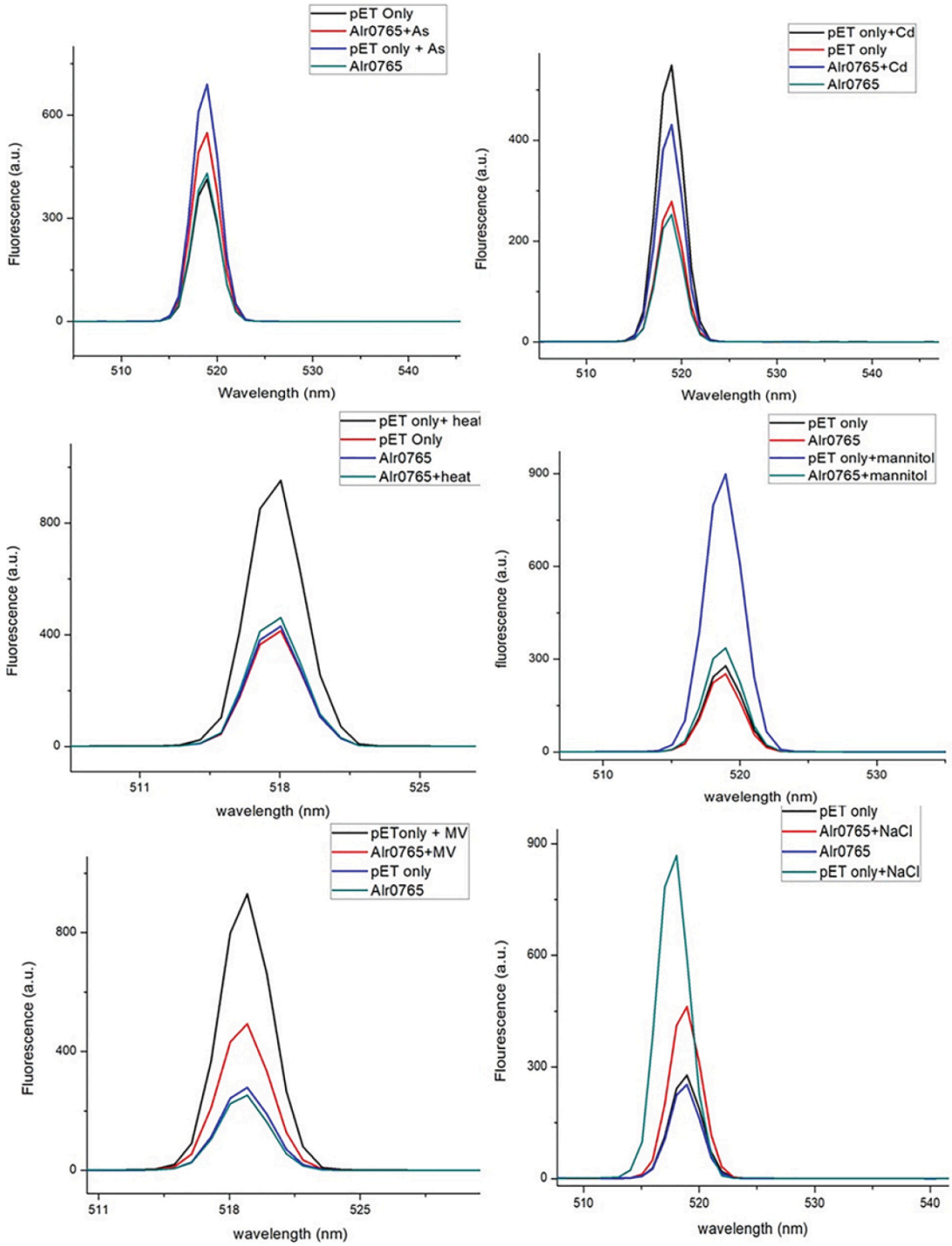

Fig. (11). Reactive oxygen species (ROS) generation analysis of *E. coli* BL21 cells carrying the empty vector (BL21/pET-21a) and recombinant vector (BL21/pET-21a-*alr0765*) under different stresses using 2,4-dichlorofluorescein diacetate (H2DCFDA). (*A higher resolution / colour version of this figure is available in the electronic copy of the article*).

(Table **3**) fall within alpha-helical, beta-sheet, turns and loops restricted to CBS domain boundary as per pdbsum and TheaDomEx (Fig. **S2**). Such findings support FTIR analysis, where variations were observed in band areas of corresponding secondary structures (Table **2**). Since CBS domain-containing proteins with AMPK activity are involved in cellular energy-sensing during stress [63] in eukaryotes, a similar function can be hypothesized for Alr0765 because of its potential to bind with different adenosyl group carrying ligands and their increased transcript level in *Anabaena* PCC7120 under different abiotic stresses. Alr0765 is unique among CBS carrying proteins because of its ability to bind with a vast range of adenosyl carrying ligands. So far, no such putative CBS has been reported to bind with ATP, ADP, AMP and NADH [64]. The only CBS-CP12 so far characterized in cyanobacteria showed binding ability with AMP only and not with other adenosyl ligands [65]. Binding with different adenosyl ligands indicates the profound ability

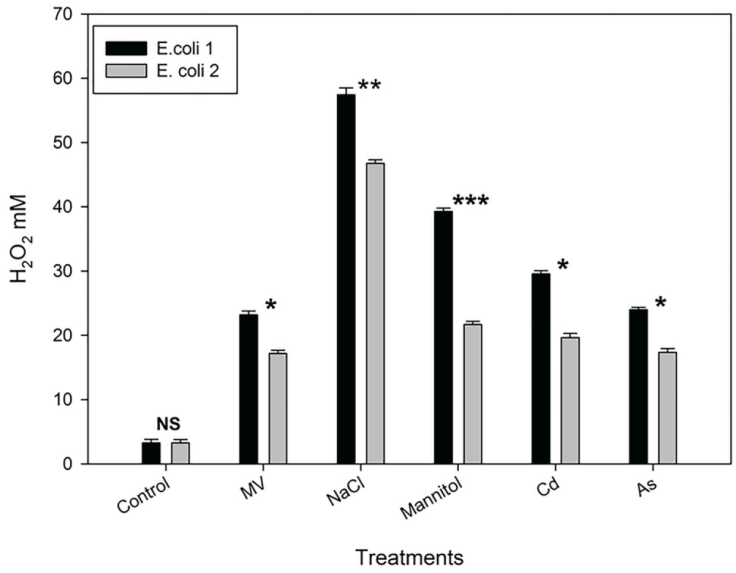

Fig. (12). H_2O_2 concentration measurement from 25 ml of each culture of BL21 transformed empty vector (*E. coli* 1) and recombinant vector (*E. coli* 2) under methyl viologen, NaCl, mannitol (dessication), cadmium and arsenic stresses showed a significant decrement in recombinant vector transformed BL21. Student's paired *t*-test (*p<0.05, **p<0.01,***p<0.001; NS not significant) was used to compare significant differences.

Table 2. Band position (cm-^{1}) and percentage area (mean+SD, n=3) corresponding to the components obtained after curve fitting of the Amide I band of Alr0765 in the absence and in the presence of 3 mM of ATP, AMP, ADP, NADH, GAPDH and PRK at pH 8.0, and 25 ^{o}C.

Secondary Structure Analysis As Determined by FTIR at 25 ^{o}C													
	Alr0765		**Alr0765+ ATP**		**Alr0765+ AMP**		**Alr0765 + ADP**		**Alr0765+ NADH**		**Alr0765+ GAPDH**		**Alr0765 +PRK**
Band Position	Band Area+-SD (%)	Band Position	Band Area+-SD (%)	Band Position	Band Area+-SD (%)	Band Position	Band Area+-SD (%)	Band Position	Band Area+-SD (%)	Band Position	Band Area+-SD (%)	Band Position	Band Area+-SD (%)
1633	13.14+0.5	1633	6.8+0.4	1633	15.52+0.1	1633	0.48+0.4	1633	19.57+0.8	1633	12.04+0.6	1633	14.23+0.3
1644	13.0 + 0.8	1644	25+1	1644	15.13+0.1	1644	431.56+ 0.238	1644	16+1	1644	11+0.3	1644	12.45+0.6
1651	4.56+0.2	1651	543.4+0.2	1651	4.57+0.3	1651	1.3+0.5	1651	208.9+0.9	1651	3.67+0.2	1651	2.64+0.3
1688	1.50+0.1	1688	9.94+0.3	1688	3.36+0.1	1688	1.1+0.3	1688	29.46+0.1	1688	2+0.1	1688	2.76+0.5

of Alr0765 to sense the cellular energy quotient. It is evident that cellular stresses cause ATP depletion, Alr0765 may be envisioned as an energy sensing module involved in switching on catabolic pathways leading to ATP synthesis and switching off the ATP consuming pathways under stress.

Microbes play an important role in the cycling of iron between the ferric and ferrous forms and generally reduce ferric iron under anaerobic conditions by using it as a final electron acceptor. To understand the involvement of iron with proteins in cellular metabolism and coping unfavorable condition, cyanobacteria are probably the best organism because of their acclaimed historical contribution in changing the earth's atmosphere from reducing to oxidizing. Iron acquisition is an essential character of cyanobacteria for maintaining a range of important physiological processes. Proteins with iron-binding ability are found to be involved in antioxidant activity towards iron-driven free radical reactions [66]. Iron acquisition property of Alr0765 is novel finding as no such reports are available for other CBS domains except for TA0289, a CBS domain fused with Zn ribbon domain in *Thermoplasma acidophilum* [67]. Iron chelating/binding proteins bear an important cellular role in the removal of free iron hence minimizing the deleterious effect produced in the reaction between ROS and Fe^{2+} in Fenton reaction in cyanobacteria [58]. Rudolf [68] reported that *Anabaena* PCC7120 produces siderophores (schizokinen) similar in structure to *E. coli* siderophores (aerobactin) involved in the uptake of Fe^{3+} *via* participation of β-barrel outer membrane proteins TonB-dependent-transporter (TBDT). Several proteins are involved in iron homeostasis, starting from its transport to

Table 3. Probable ligands with consensus binding residues of Alr0765 as revealed with COAH.

Ligand Name	Consensus Binding Residue
ATP	Met^{8},Lys^{10},Asp^{11},Val^{12},Asp^{32},Trp^{33},Arg^{34},Leu^{36},His^{101},Gly^{112},Ile^{114},Ser^{115},Leu116,Thr^{117}
AMP	Met^{8}, Ile^{50},Glu^{52},Ser^{53},Met^{75},Lys^{77},Pro^{78},Cys^{79},Gly^{99},Leu^{100},His^{101},Ala^{103}
NADH	Ser^{53}, Phe^{95}, Ala^{96}, Gly^{99}, Leu^{100}, His^{101}, Leu^{116}
Fe^{2+}	Cys^{149}, Thr^{152}, Asn^{155}, Glu^{172}, Val^{181}, Thr^{184}

binding to iron-dependent regulators to sequestration. The Association of iron with isolated Alr0765 has been corroborated by AAS data and EDS spectrum (Fig. **11**). A significant abundance in the transcript level of *alr0765* from *Anabaena* PCC7120 exposed to different concentrations of $FeCl_3$ attested its involvement in iron acquisition (Fig. **10**). In addition, the downshift in transcript level under increasing iron exposure of cells suggests that at lower concentration (0.1µM and 0.5µM), the target protein is able to tightly regulate the cellular level of iron although at higher concentration (1µM, 3µM, and 5µM), free iron becomes toxic to cell leading to ROS production and finally protein degradation. qRT PCR also suggested a higher transcript level of *alr0765* in the presence of iron in the medium as compared to medium without iron after induction with IPTG (Fig. **S7**). Moreover, Alr0765 comprises peptide motif E-X-X-E responsible for iron-binding [69] as $E^{192}Y^{193}P^{194}E^{195}A^{196}L^{197}E^{198}$ sequence stretch. Protein involved in iron binding or storage bears the utmost importance under oxidative stress *via* protecting cells from free ferrous forms, thus prevents the production of ROS *via* Fenton reaction. Studies show that by sequestering of excess free iron, iron storage proteins protected *Pseudomonas aeruginosa* and *Brucella abortus* against hydrogen peroxide [70, 71]. Mutation in two iron storage proteins bfrA and bfrB from *Mycobacterium tuberculosis* drastically reduced their capacity to tolerate abiotic stress [72]. A decrease in ROS and H_2O_2 cellular level of recombinant vector transformed *E. coli* compared to empty vector transformed *E. coli* under different stresses supported such assumptions (Figs. **6** and **7**). In contrast to this, iron is an essential component present in heme, iron sulphur protein, cofactor for several enzymes involved in various cellular processes hence crucial for growth, particularly for photosynthetic organisms.

The presence of CP12 domain in Alr0765 indicated the redox sensitivity of the target protein as elucidated by redox potential generated, 146 mV measured with cyclic voltammetry (Fig. **12**). The redox potential generated felled between the standard physiological E° (~ -1V, at which protons are reduced to H_2, and 1V, at which water is oxidized to O_2) [73] and comparable to different metalloproteins such as high potential iron-sulphur proteins (HiPIPs) (100-500mV) [74]. This finding suggested that Alr0765 involved in bioenergetic processes in the cell is playing a crucial role in electron transfer reaction between different redox partners.

Alr0765 is not involved in GAPDH/CP12/PRK complex formation, the very common role assigned to CP12 proteins [75] as no interaction profiles of Alr0765 with GAPDH as well as PRK was observed with FTIR spectra (Table **2**). Such findings are in agreement with the findings of Hackenberg *et al.*, [65] on CBS-CP12 fusion protein from bloom-forming cyanobacterium where no involvement in GAPDH/ CP12/PRK complex formation was noticed. Stanley [2] also reported that CBS-CP12 fusion proteins are not able to interact with GAPDH, as observed by *in silico* analysis. This can be correlated with the fact that Alr0765 does not possess a C terminal cysteine pair hence lacking two intramolecular disulphide bridges (the N and C terminal cysteine pairs with respect to core "AWD_VEEL") which on oxidation converted into thiol groups after reduction by thioredoxin. Moreover, like Alr0765, the other proteins with CBS-CP12 domains in *Anabaena* PCC7120 co-expressed with non-photosynthetic genes like hox-type hydrogenase [76] and *nif* gene cluster [77] hence the neighborhood is also unrelated to photosynthesis thus denies their involvement in carbon fixation. In *Arabidopsis thaliana* under oxidative stress, CP12 influenced the dimerization of CBSX1 protein localized in chloroplast resulting in an increased level of reduced thioredoxin and hence CP12 maintained in the reduced state [11]. Although ESI/MS analysis of native Alr0765 confirmed its dimerization (Fig. **4**), the role of CP12 might be to hold tight regulation of alteration in redox status of the cell under abiotic stresses.

CONCLUSION

The present study suggests that in view of the multiple functions of Alr0765, it may be assumed to be a moonlighting protein having critical involvement in abiotic stress management by *Anabaena* PCC7120. Hence, Alr0765 is a potential candidate for the development of transgenic lines both in cyanobacteria as well as higher plants endowed with multiple abiotic stress tolerance.

AUTHORS' CONTRIBUTIONS

Antra Chatterjee designed the experiment, conducted the experiments and wrote the manuscript. Shilpi Singh, Ruchi Rai, and Shweta Rai, helped in performing different experiments and *in-silico* analysis. L.C. Rai gave guidance throughout the research work and critically reviewed the manuscript.

ETHICS APPROVAL AND CONSENT TO PARTICIPATE

Not applicable.

HUMAN AND ANIMAL RIGHTS

No Animals/Humans were used for studies that are the basis of this research.

CONSENT FOR PUBLICATION

Not applicable.

AVAILABILITY OF DATA AND MATERIALS

The data supporting the findings of the article is available in the [KEGG] at [https://www.genome.jp/dbget-bin/www_bget?ana:alr0765], reference number [T00069]. Model organism Anabaena sp. PCC7120 has whole-genome sequenced, including hypothetical protein Alr0765 accession number WP_010994939.1.

FUNDING

L.C. Rai thanks the Indian Council of Agricultural Research-National Bureau of Agriculturally Important Microorganisms (ICAR-NBAIM), (Grant number NBAIM/AMAAS/2014-15/36), for financial support. DST, (DST-EMR/2017/001343), J.C. Bose National Fellowship (SR/S02/JCB- 73/09) and DAE for Raja Ramanna for Fellowships (DAE/2016/P-29/92) respectively. Antra Chatterjee is thankful to the University Grants Commission (UGC) for SRF. Shweta Rai is thankful to CSIR for Senior Research Fellowship (SRF). Shilpi Singh and Ruchi Rai thank UGC for Dr. D.S. Kothari postdoctoral research fellowship and DST, New Delhi for Women Scientist Scheme A (WOSA) award, respectively.

CONFLICT OF INTEREST

The authors declare no conflict of interest, financial or otherwise.

ACKNOWLEDGEMENTS

Declared none.

SUPPLEMENTARY MATERIAL

Supplementary material is available on the publisher's website along with the published article.

REFERENCES

[1] Babele, P.K.; Kumar, J.; Chaturvedi, V. Proteomic de-regulation in cyanobacteria in response to abiotic stresses. *Front. Microbiol.,* **2019**, *10*, 1315. http://dx.doi.org/10.3389/fmicb.2019.01315 PMID: 31263458

[2] Stanley, D.N.; Raines, C.A.; Kerfeld, C.A. Comparative analysis of 126 cyanobacterial genomes reveals evidence of functional diversity among homologs of the redox-regulated CP12 protein. *Plant Physiol.,* **2013**, *161*(2), 824-835. http://dx.doi.org/10.1104/pp.112.210542 PMID: 23184231

[3] Scott, J.W.; Hawley, S.A.; Green, K.A.; Anis, M.; Stewart, G.; Scullion, G.A.; Norman, D.G.; Hardie, D.G. CBS domains form energy-sensing modules whose binding of adenosine ligands is disrupted by disease mutations. *J. Clin. Invest.,* **2004**, *113*(2), 274-284. http://dx.doi.org/10.1172/JCI19874 PMID: 14722619

[4] Biemans-Oldehinkel, E.; Mahmood, N.A.B.; Poolman, B. A sensor for intracellular ionic strength. *Proc. Natl. Acad. Sci. USA,* **2006**, *103*(28), 10624-10629. http://dx.doi.org/10.1073/pnas.0603871103 PMID: 16815971

[5] Ishitani, R.; Sugita, Y.; Dohmae, N.; Furuya, N.; Hattori, M.; Nureki, O. Mg^{2+}-sensing mechanism of Mg^{2+} transporter MgtE probed by molecular dynamics study. *Proc. Natl. Acad. Sci. USA,* **2008**, *105*(40), 15393-15398. http://dx.doi.org/10.1073/pnas.0802991105 PMID: 18832160

[6] Carr, G.; Simmons, N.; Sayer, J. A role for CBS domain 2 in trafficking of chloride channel CLC-5. *Biochem. Biophys. Res. Commun.,* **2003**, *310*(2), 600-605. http://dx.doi.org/10.1016/j.bbrc.2003.09.057 PMID: 14521953

[7] De, A.A.; Moran, O.; Wege, S.; Filleur, S.; Ephritikhine, G.; Thomine, S.; Barbier-Brygoo, H.; Gambale, F. ATP binding to the C terminus of the *Arabidopsis thaliana* nitrate/proton antiporter, AtCLCa, regulates nitrate transport into plant vacuoles. *J. Biol. Chem.,* **2009**, *284*, 26526-26532. http://dx.doi.org/10.1074/jbc.M109.005132

[8] Tuominen, H.; Salminen, A.; Oksanen, E.; Jämsen, J.; Heikkilä, O.; Lehtiö, L.; Magretova, N.N.; Goldman, A.; Baykov, A.A.; Lahti, R. Crystal structures of the CBS and DRTGG domains of the regulatory region of *Clostridiumperfringens* pyrophosphatase complexed with the inhibitor, AMP, and activator, diadenosine tetraphosphate. *J. Mol. Biol.,* **2010**, *398*(3), 400-413. http://dx.doi.org/10.1016/j.jmb.2010.03.019 PMID: 20303981

[9] Bateman, A. The structure of a domain common to archaebacteria and the homocystinuria disease protein. *Trends Biochem. Sci.,* **1997**, *22*(1), 12-13. http://dx.doi.org/10.1016/S0968-0004(96)30046-7 PMID: 9020585

[10] Kushwaha, H.R.; Singh, A.K.; Sopory, S.K.; Singla-Pareek, S.L.; Pareek, A. Genome wide expression analysis of CBS domain containing proteins in *Arabidopsis thaliana* (L.) Heynh and *Oryza sativa L.* reveals their developmental and stress regulation. *BMC Genomics,* **2009**, *10*, 200. http://dx.doi.org/10.1186/1471-2164-10-200 PMID: 19400948

[11] Yoo, K.S.; Ok, S.H.; Jeong, B.C.; Jung, K.W.; Cui, M.H.; Hyoung, S.; Lee, M.R.; Song, H.K.; Shin, J.S. Single cystathionine β-synthase domain-containing proteins modulate development by regulating the thioredoxin system in *Arabidopsis. Plant Cell,* **2011**, *23*(10), 3577-3594. http://dx.doi.org/10.1105/tpc.111.089847 PMID: 22021414

[12] Singh, A.K.; Kumar, R.; Pareek, A.; Sopory, S.K.; Singla-Pareek, S.L. Overexpression of rice CBS domain containing protein improves salinity, oxidative, and heavy metal tolerance in transgenic tobacco. *Mol. Biotechnol.,* **2012**, *52*(3), 205-216. http://dx.doi.org/10.1007/s12033-011-9487-2 PMID: 22302312

[13] Wang, X.; Ren, X.; Zhu, L.; He, G. A rice gene, encodes a novel protein with a CBS-like domain and its expression is induced in responses to herbivore feeding. *Plant Sci.,* **2004**, *166*, 1581-1588. http://dx.doi.org/10.1016/j.plantsci.2004.02.011

[14] Wedel, N.; Soll, J.; Paap, B.K. CP12 provides a new mode of light regulation of Calvin cycle activity in higher plants. *Proc. Natl. Acad. Sci. USA,* **1997**, *94*(19), 10479-10484. http://dx.doi.org/10.1073/pnas.94.19.10479 PMID: 9294236

[15] Erales, J.; Gontero, B.; Maberly, S.C. Specificity and function of glyceraldehyde-3phosphate dehydrogenase in a freshwater diatom, *Asterionella formosa* (Bacillariophyceae). *J. Phycol.,* **2008**, *44*(6), 1455-1464. http://dx.doi.org/10.1111/j.1529-8817.2008.00600.x PMID: 27039860

[16] Groben, R.; Kaloudas, D.; Raines, C.A.; Offmann, B.; Maberly, S.C.; Gontero, B. Comparative sequence analysis of CP12, a small protein involved in the formation of a Calvin cycle complex in photosynthetic organisms. *Photosynth. Res.,* **2010**, *103*(3), 183-194. http://dx.doi.org/10.1007/s11120-010-9542-z PMID: 20224939

[17] Marri, L.; Trost, P.; Pupillo, P.; Sparla, F. Reconstitution and properties of the recombinant glyceraldehyde-3-phosphate dehydrogenase/CP12/phosphoribulokinase supramolecular complex of *Arabidopsis. Plant Physiol.,* **2005**, *139*(3), 1433-1443. http://dx.doi.org/10.1104/pp.105.068445 PMID: 16258009

[18] Marri, L.; Zaffagnini, M.; Collin, V.; Issakidis-Bourguet, E.; Lemaire, S.D.; Pupillo, P.; Sparla, F.; Miginiac-Maslow, M.; Trost, P. Prompt and easy activation by specific thioredoxins of calvin cycle enzymes of *Arabidopsis thaliana* associated in the GAPDH/CP12/PRK supramolecular complex. *Mol. Plant,* **2009**, *2*(2), 259-269. http://dx.doi.org/10.1093/mp/ssn061 PMID: 19825612

[19] Buchanan, B.B.; Balmer, Y. Redox regulation: a broadening horizon. *Annu. Rev. Plant Biol.,* **2005**, *56*, 187-220.

http://dx.doi.org/10.1146/annurev.arplant.56.032604.144246 PMID: 15862094

[20] Marri, L.; Thieulin-Pardo, G.; Lebrun, R.; Puppo, R.; Zaffagnini, M.; Trost, P.; Gontero, B.; Sparla, F. CP12-mediated protection of Calvin-Benson cycle enzymes from oxidative stress. *Biochimie,* **2014**, *97*, 228-237. http://dx.doi.org/10.1016/j.biochi.2013.10.018 PMID: 24211189

[21] Rai, L.C.; Kumar, H.D.; Mohn, F.H.; Soeder, C.J. Services of algae to the environment. *J. Microbiol. Biotechnol.,* **2000**, *10*, 119-136.

[22] Shcolnick, S.; Shaked, Y.; Keren, N. A role for mrgA, a DPS family protein, in the internal transport of Fe in the cyanobacterium *Synechocystis* sp. PCC6803. *Biochim. Biophys. Acta,* **2007**, *1767*(6), 814-819. http://dx.doi.org/10.1016/j.bbabio.2006.11.015 PMID: 17234153

[23] Holden, V.I.; Wright, M.S.; Houle, S.; Collingwood, A.; Dozois, C.M.; Adams, M.D.; Bachman, M.A. Iron acquisition and siderophore release by carbapenem-resistant sequence type 258 *Klebsiella pneumonia. MSphere,* **2018**, *3*(2), e00125-e18. http://dx.doi.org/10.1128/mSphere.00125-18 PMID: 29669884

[24] Pandey, S.; Rai, R.; Rai, L.C. Proteomics combines morphological, physiological and biochemical attributes to unravel the survival strategy of Anabaena sp. PCC7120 under arsenic stress. *J. Proteomics,* **2012**, *75*(3), 921-937. http://dx.doi.org/10.1016/j.jprot.2011.10.011 PMID: 22057044

[25] Rai, S.; Agrawal, C.; Shrivastava, A.K.; Singh, P.K.; Rai, L.C. Comparative proteomics unveils cross species variations in *Anabaena* under salt stress. *J. Proteomics,* **2014**, *98*, 254-270. http://dx.doi.org/10.1016/j.jprot.2013.12.020 PMID: 24406298

[26] Rajaram, H.; Apte, S.K. Nitrogen status and heat-stress-dependent differential expression of the cpn60 chaperonin gene influences thermotolerance in the cyanobacterium *Anabaena. Microbiology,* **2008**, *154*(Pt 1), 317-325. http://dx.doi.org/10.1099/mic.0.2007/011064-0 PMID: 18174150

[27] Shrivastava, A.K.; Chatterjee, A.; Yadav, S.; Singh, P.K.; Singh, S.; Rai, L.C. UV-B stress induced metabolic rearrangements explored with comparative proteomics in three *Anabaena s*pecies. *J. Proteomics,* **2015**, *127*(Pt A), 122-133. http://dx.doi.org/10.1016/j.jprot.2015.05.014 PMID: 25997677

[28] Sen, S.; Rai, S.; Yadav, S.; Agrawal, C.; Rai, R.; Chatterjee, A.; Rai, L.C. Dehydration and rehydration-induced temporal changes in cytosolic and membrane proteome of the nitrogen fixing cyanobacterium *Anabaena* PCC7120. *Algal Res.,* **2017**, *27*, 244-258. http://dx.doi.org/10.1016/j.algal.2017.09.012

[29] Agrawal, C.; Sen, S.; Singh, S.; Rai, S.; Singh, P.K.; Singh, V.K.; Rai, L.C. Comparative proteomics reveals association of early accumulated proteins in conferring butachlor tolerance in three N(2)-fixing Anabaena spp. *J. Proteomics,* **2014**, *96*, 271-290. http://dx.doi.org/10.1016/j.jprot.2013.11.015 PMID: 24291601

[30] Singh, P.K.; Shrivastava, A.K.; Chatterjee, A.; Pandey, S.; Rai, S.; Singh, S.; Rai, L.C. Cadmium toxicity in diazotrophic *Anabaena* spp. adjudged by hasty up-accumulation of transporter and signaling and severe down-accumulation of nitrogen metabolism proteins. *J. Proteomics,* **2015**, *127*(Pt A), 134-146. http://dx.doi.org/10.1016/j.jprot.2015.05.019 PMID: 26021478

[31] Panda, B.; Basu, B.; Rajaram, H.; Apte, S.K. Comparative proteomics of oxidative stress response in three cyanobacterial strains native to Indian paddy fields. *J. Proteomics,* **2015**, *127*(Pt A), 152-160. http://dx.doi.org/10.1016/j.jprot.2015.05.020 PMID: 26013413

[32] Chaurasia, N.; Mishra, Y.; Chatterjee, A.; Rai, R.; Yadav, S.; Rai, L.C. Overexpression of phytochelatin synthase (pcs) enhances abiotic stress tolerance by altering the proteome of transformed *Anabaena* sp. PCC 7120. *Protoplasma,* **2017**, *254*(4), 1715-1724. http://dx.doi.org/10.1007/s00709-016-1059-7 PMID: 28000119

[33] Banerjee, S.; Mazumdar, S. Electrospray ionization mass spectrometry: a technique to access the information beyond the molecular weight of the analyte. *Int. J. Anal. Chem.,* **2012**, *2012,* 282574. http://dx.doi.org/10.1155/2012/282574 PMID: 22611397

[34] Martínez-Cruz, L.A.; Encinar, J.A.; Sevilla, P.; Oyenarte, I.; Gómez-García, I.; Aguado-Llera, D.; García-Blanco, F.; Gómez, J.; Neira, J.L. Nucleotide-induced conformational transitions in the CBS domain protein MJ0729 of *Methanocaldococcus jannaschii. Protein Eng. Des. Sel.,* **2011**, *24*(1-2), 161-169. http://dx.doi.org/10.1093/protein/gzq073 PMID: 20959390

[35] Bates, S.S.; Tessier, A.; Campbell, P.G.C.; Buffle, J. Zinc adsorption and transport by *Chlamydomonas variabilis* and *Scenedesmus subspicatus* (Chlorophyceae) grown in semicontinuous culture. *J. Phycol.,* **1982**, *18*, 521-529. http://dx.doi.org/10.1111/j.1529-8817.1982.tb03218.x

[36] Nishio, K.; Pornpitra, T.; Izawa, S.; Nishiwaki-Ohkawa, T.; Kato, S.; Hashimoto, K.; Nakanishi, S. Electrochemical detection of circadian redox rhythm in cyanobacterial cells *via* extracellular electron transfer. *Plant Cell Physiol.,* **2015**, *56*(6), 1053-1058. http://dx.doi.org/10.1093/pcp/pcv066 PMID: 25975263

[37] Jakubowski, W.; Bartosz, G. 2,7-dichlorofluorescin oxidation and reactive oxygen species: what does it measure? *Cell Biol. Int.,* **2000**, *24*(10), 757-760. http://dx.doi.org/10.1006/cbir.2000.0556 PMID: 11023655

[38] Rao, M.V.; Paliyath, G.; Ormrod, D.P.; Murr, D.P.; Watkins, C.B. Influence of salicylic acid on H_2O_2 production, oxidative stress, and H_2O_2-metabolizing enzymes. Salicylic acid-mediated oxidative damage requires H_2O_2. *Plant Physiol.,* **1997**, *115*(1), 137-149. http://dx.doi.org/10.1104/pp.115.1.137 PMID: 9306697

[39] Agrawal, C.; Sen, S.; Yadav, S.; Rai, S.; Rai, L.C. A novel aldoketoreductase (AKR17A1) of *Anabaena* PCC7120 degrades the rice field herbicide butachlor and confers abiotic stress tolerance in *E. coli*. *PLoS One,* **2015**, *10,* 0137744. http://dx.doi.org/10.1371/journal.pone.0137744

[40] Zdobnov, E.M.; Apweiler, R. InterProScan--an integration platform for the signature-recognition methods in InterPro. *Bioinformatics,* **2001**, *17*(9), 847-848. http://dx.doi.org/10.1093/bioinformatics/17.9.847 PMID: 11590104

[41] Zhang, C.; Freddolino, P.L.; Zhang, Y. COFACTOR: improved protein function prediction by combining structure, sequence and protein-protein interaction information. *Nucleic Acids Res.,* **2017**, *45*(W1), W291-W299. http://dx.doi.org/10.1093/nar/gkx366 PMID: 28472402

[42] Yang, J.; Roy, A.; Zhang, Y. BioLiP: a semi-manually curated database for biologically relevant ligand-protein interactions. *Nucleic Acids Res.,* **2013**, *41*(Database issue), D1096-D1103. PMID: 23087378

[43] Rost, B.; Yachdav, G.; Liu, J. The predict protein server. *Nucleic Acids Res.,* **2004**, *32 (Web Server issue)*, W321-W326.

[44] Biasini, M.; Bienert, S.; Waterhouse, A.; Arnold, K.; Studer, G.; Schmidt, T.; Kiefer, F.; Gallo Cassarino, T.; Bertoni, M.; Bordoli, L.; Schwede, T. SWISS-MODEL: modelling protein tertiary and quaternary structure using evolutionary information. *Nucleic Acids Res.,* **2014**, *42*(Web Server issue), W252-W258. http://dx.doi.org/10.1093/nar/gku340 PMID: 24782522

[45] Xu, D.; Zhang, Y. Improving the physical realism and structural accuracy of protein models by a two-step atomic-level energy minimization. *Biophys. J.,* **2011**, *101*(10), 2525-2534. http://dx.doi.org/10.1016/j.bpj.2011.10.024 PMID: 22098752

[46] Laskowski, R.A.; MacArthur, M.W.; Moss, D.S.; Thornton, J.M. PROCHECK-A program to check the stereochemical quality of protein structures. *J. Appl. Cryst.,* **1993**, *26*, 283-291. http://dx.doi.org/10.1107/S0021889892009944

[47] Colovos, C.; Yeates, T.O. Verification of protein structures: patterns of nonbonded atomic interactions. *Protein Sci.,* **1993**, *2*(9), 1511-1519. http://dx.doi.org/10.1002/pro.5560020916 PMID: 8401235

[48] Davis, I.W.; Leaver-Fay, A.; Chen, V.B.; Block, J.N.; Kapral, G.J.; Wang, X.; Murray, L.W.; Arendall, W.B., III; Snoeyink, J.; Richardson, J.S.; Richardson, D.C. MolProbity: all-atom contacts and structure validation for proteins and nucleic acids. *Nucleic Acids Res.,* **2007**, *35*(Web Server issue), W375-W383. http://dx.doi.org/10.1093/nar/gkm216 PMID: 17452350

[49] Wiederstein, M.; Sippl, M.J. ProSA-web: interactive web service for the recognition of errors in three-dimensional structures of proteins. *Nucleic Acids Res.,* **2007**, *35*(Web Server issue), W407-W410. http://dx.doi.org/10.1093/nar/gkm290 PMID: 17517781

[50] Zhang, Y.; Skolnick, J. TM-align: a protein structure alignment algorithm based on the TM-score. *Nucleic Acids Res.,* **2005**, *33*(7), 2302-2309. http://dx.doi.org/10.1093/nar/gki524 PMID: 15849316

[51] Day, P.; Sharff, A.; Parra, L.; Cleasby, A.; Williams, M.; Hörer, S.; Nar, H.; Redemann, N.; Tickle, I.; Yon, J. Structure of a CBS-domain pair from the regulatory gamma1 subunit of human AMPK

in complex with AMP and ZMP. *Acta Crystallogr. D Biol. Crystallogr.,* **2007**, *63*(Pt 5), 587-596. http://dx.doi.org/10.1107/S0907444907009110 PMID: 17452784

[52] Soti, C.; Vermes, A.; Haystead, T.A.; Csermely, P. Comparative analysis of the ATP-binding sites of Hsp90 by nucleotide affinity cleavage: a distinct nucleotide specificity of the C-terminal ATP-binding site. *Eur. J. Biochem.,* **2003**, *270*(11), 2421-2428. http://dx.doi.org/10.1046/j.1432-1033.2003.03610.x PMID: 12755697

[53] Hiratsuka, T. Fluorescent and colored trinitrophenylated analogs of ATP and GTP. *Eur. J. Biochem.,* **2003**, *270*(17), 3479-3485. http://dx.doi.org/10.1046/j.1432-1033.2003.03748.x PMID: 12919312

[54] Plesniak, L.; Horiuchi, Y.; Sem, D.; Meinenger, D.; Stiles, L.; Shaffer, J.; Jennings, P.A.; Adams, J.A. Probing the nucleotide binding domain of the osmoregulator EnvZ using fluorescent nucleotide derivatives. *Biochemistry,* **2002**, *41*(47), 13876-13882. http://dx.doi.org/10.1021/bi020331j PMID: 12437344

[55] Kong, J.; Yu, S. Fourier transform infrared spectroscopic analysis of protein secondary structures. *Acta Biochim. Biophys. Sin. (Shanghai),* **2007**, *39*(8), 549-559. http://dx.doi.org/10.1111/j.1745-7270.2007.00320.x PMID: 17687489

[56] Banyay, M.; Sarkar, M.; Gräslund, A. A library of IR bands of nucleic acids in solution. *Biophys. Chem.,* **2003**, *104*(2), 477-488. http://dx.doi.org/10.1016/S0301-4622(03)00035-8 PMID: 12878315

[57] Wang, Y.; Wang, J.; Li, R.; Shi, Q.; Xue, Z.; Zhang, Y. ThreaDomEx: a unified platform for predicting continuous and discontinuous protein domains by multiple-threading and segment assembly. *Nucleic Acids Res.,* **2017**, *45*(W1), W400-W407. http://dx.doi.org/10.1093/nar/gkx410 PMID: 28498994

[58] Shcolnick, S.; Summerfield, T.C.; Reytman, L.; Sherman, L.A.; Keren, N. The mechanism of iron homeostasis in the unicellular cyanobacterium *synechocystis s*p. PCC 6803 and its relationship to oxidative stress. *Plant Physiol.,* **2009**, *150*(4), 2045-2056. http://dx.doi.org/10.1104/pp.109.141853 PMID: 19561120

[59] Kemp, B.E. Bateman domains and adenosine derivatives form a binding contract. *J. Clin. Invest.,* **2004**, *113*(2), 182-184. http://dx.doi.org/10.1172/JCI200420846 PMID: 14722609

[60] Lucas, M.; Encinar, J.A.; Arribas, E.A.; Oyenarte, I.; García, I.G.; Kortazar, D.; Ferna'ndez, J.A.; Mato, J.M.; Martínez-Chantar, M.L.; Martínez-Cruz, L.A. Cystathionine β-Synthase (CBS) Domains 1 and 2 fulfill different roles in ionic strength sensing of the ATP-binding cassette (ABC) transporter OpuA. *J. Mol. Biol.,* **2010**, *396*, 800-820. http://dx.doi.org/10.1016/j.jmb.2009.12.012 PMID: 20026078

[61] Hardie, D.G.; Scott, J.W.; Pan, D.A.; Hudson, E.R. Management of cellular energy by the AMP-activated protein kinase system. *FEBS Lett.,* **2003**, *546*(1), 113-120. http://dx.doi.org/10.1016/S0014-5793(03)00560-X PMID: 12829246

[62] Léger, C.; Elliott, S.J.; Hoke, K.R.; Jeuken, L.J.C.; Jones, A.K.; Armstrong, F.A. Enzyme electrokinetics: using protein film voltammetry to investigate redox enzymes and their mechanisms. *Biochemistry,* **2003**, *42*(29), 8653-8662. http://dx.doi.org/10.1021/bi034789c PMID: 12873124

[63] Hardie, D.G.; Hawley, S.A. AMP-activated protein kinase: the energy charge hypothesis revisited. *BioEssays,* **2001**, *23*(12), 1112-1119. http://dx.doi.org/10.1002/bies.10009 PMID: 11746230

[64] Ereño-Orbea, J.; Oyenarte, I.; Martínez-Cruz, L.A. CBS domains: ligand binding sites and conformational variability. *Arch. Biochem. Biophys.,* **2013**, *540*(1-2), 70-81. http://dx.doi.org/10.1016/j.abb.2013.10.008 PMID: 24161944

[65] Hackenberg, C.; Hakanpää, J.; Cai, F.; Antonyuk, S.; Eigner, C.; Meissner, S.; Laitaoja, M.; Jänis, J.; Kerfeld, C.A.; Dittmann, E.; Lamzin, V.S. Structural and functional insights into the unique CBS-CP12 fusion protein family in cyanobacteria. *Proc. Natl. Acad. Sci. USA,* **2018**, *115*(27), 7141-7146. http://dx.doi.org/10.1073/pnas.1806668115 PMID: 29915055

[66] Gutteridge, J.M.C.; Halliwell, B. Mini-review: oxidative stress, redox stress or redox success? *Biochem. Biophys. Res. Commun.,* **2018**, *502*(2), 183-186. http://dx.doi.org/10.1016/j.bbrc.2018.05.045 PMID: 29752940

[67] Proudfoot, M.; Sanders, S.A.; Singer, A.; Zhang, R.; Brown, G.; Binkowski, A.; Xu, L.; Lukin, J.A.; Murzin, A.G.; Joachimiak, A.; Arrowsmith, C.H.; Edwards, A.M.; Savchenko, A.V.; Yakunin, A.F. Biochemical and structural characterization of a novel family of cystathionine beta-synthase domain proteins fused to a Zn ribbon-like domain. *J. Mol. Biol.,* **2008**, *375*(1), 301-315. http://dx.doi.org/10.1016/j.jmb.2007.10.060 PMID: 18021800

[68] Rudolf, M.; Kranzler, C.; Lis, H.; Margulis, K.; Stevanovic, M.; Keren, N.; Schleiff, E. Multiple modes of iron uptake by the filamentous, siderophore-producing cyanobacterium, *Anabaena* sp. PCC 7120. *Mol. Microbiol.,* **2015**, *97*(3), 577-588. http://dx.doi.org/10.1111/mmi.13049 PMID: 25943160

[69] Fang, H.M.; Wang, Y. Characterization of iron-binding motifs in *Candida albicans* high-affinity iron permease CaFtr1p by site-directed mutagenesis. *Biochem. J.,* **2002**, *368*(Pt 2), 641-647. http://dx.doi.org/10.1042/bj20021005 PMID: 12207560

[70] Ma, J.F.; Ochsner, U.A.; Klotz, M.G.; Nanayakkara, V.K.; Howell, M.L.; Johnson, Z.; Posey, J.E.; Vasil, M.L.; Monaco, J.J.; Hassett, D.J. Bacterioferritin A modulates catalase A (KatA) activity and resistance to hydrogen peroxide in *Pseudomonas aeruginosa. J. Bacteriol.,* **1999**, *181*(12), 3730-3742. http://dx.doi.org/10.1128/JB.181.12.3730-3742.1999 PMID: 10368148

[71] Almirón, M.A.; Ugalde, R.A. Iron homeostasis in *Brucella abortus*: the role of bacterioferritin. *J. Microbiol.,* **2010**, *48*(5), 668-673. http://dx.doi.org/10.1007/s12275-010-0145-3 PMID: 21046346

[72] Reddy, P.V.; Puri, R.V.; Khera, A.; Tyagi, A.K. Iron storage proteins are essential for the survival and pathogenesis of *Mycobacterium tuberculosis* in THP-1 macrophages and the guinea pig model of infection. *J. Bacteriol.,* **2012**, *194*(3), 567-575. http://dx.doi.org/10.1128/JB.05553-11 PMID: 22101841

[73] Hosseinzadeh, P.; Lu, Y. Design and fine-tuning redox potentials of metalloproteins involved in electron transfer in bioenergetics. *Biochim. Biophys. Acta,* **2016**, *1857*(5), 557-581. http://dx.doi.org/10.1016/j.bbabio.2015.08.006 PMID: 26301482

[74] Lu, Y. Electron transfer: Cupredoxins, In: *Biocoordination Chemistry*; J.L, Que.; W.B. , Tolman., Eds.; Elsevier, Oxford, UK, **2004**, pp. 91 -122. [8] D.B. Rorabacher, Electron Transfer by Copper Centers, Chem. Rev., *104*(2004). 651-698.

[75] Lopez-Calcagno, P.E.; Howard, T.P.; Raines, C.A. The CP-12 protein family: a thioredoxin metabolic switch? *Front. Plant Sci.,* **2014**, *5*, 1-9. http://dx.doi.org/10.3389/fpls.2014.00009

[76] Sjöholm, J.; Oliveira, P.; Lindblad, P. Transcription and regulation of the bidirectional hydrogenase in the cyanobacterium *Nostoc* sp. strain PCC 7120. *Appl. Environ. Microbiol.,* **2007**, *73*(17), 5435-5446. http://dx.doi.org/10.1128/AEM.00756-07 PMID: 17630298

[77] Ehira, S.; Ohmori, M.; Sato, N. Genome-wide expression analysis of the responses to nitrogen deprivation in the heterocyst-forming cyanobacterium *Anabaena* sp. strain PCC 7120. *DNA Res.,* **2003**, *10*(3), 97-113. http://dx.doi.org/10.1093/dnares/10.3.97 PMID: 12886952